# Challenges in Application of Distance Relays under Power Swing Conditions

Zhiying Zhang, Anil Jacques, Ilia Voloh - GE Grid Solutions, Markham, ON, Canada

*Abstract:*

**Power system disturbances may cause stable or unstable power swings in the system. As a result, apparent impedance trajectories could enter into distance characteristics during a power swing and cause distance relay mis-operation. A power swing blocking (PSB) function is typically included in modern distance relays to block distance elements from undesired operation due to a power swing.**

**However, the blocking signal (from PSB) to the distance elements needs to be removed when a line fault (either unbalanced or balanced) occurs at any time during the swing so that the distance elements are able to clear the legitimate line fault. After the removal of the PSB signal from the distance elements, dependability, security and selectivity of the distance elements should be maintained.**

**Such requirements have brought some difficulties to the distance relay in certain applications, including, ensuring the valid operating condition of various distance comparators with signal variation (magnitude, phase and frequency) caused by a power swing, detecting faults and properly removing PSB blocking without causing security issues, and making settings adaptable to the changing conditions while at the same time meeting the above mentioned requirements.**

**In this paper, we will start with a theoretical analysis of the power swing condition, especially focusing on how signals supplied to the relay would vary during power swing conditions, in terms of magnitude, phase and frequency. Based on the analysis, we will investigate how the digital distance relay performance could be affected with such signals and varying conditions. After that, solutions to overcome the limiting conditions and avoid mal-operations, combined with a recent application of the distance relays in Asia, will be discussed. Results and conclusions are supported by PSCAD and RTDS simulation testing.**

*Keywords*: **Power Swing, Distance Protection, Power Swing Blocking (PSB), Out of Step (OOS), Memory Polarization, Self-Polarization, Frequency Tracking.**

## I. INTRODUCTION

In the stable state of the power system operation condition, power generation and load are balanced, and all generators in the network rotate with the same speed. Disturbances in the system, such as faults, connection or disconnection of loads or generators, or changes in the system configurations, may upset the balance between generation and load, and result in generator rotor angle oscillations. Some generators may accelerate and some generators may decelerate and cause power flow swings in the system.

Depending on the severity of the disturbance and system conditions, these power swings can be stable or unstable. During stable swings, machines will settle to a new stable state, in which synchronism among generators in the network is retained. During unstable swings, synchronism cannot be maintained, and some generators run out of step (OOS).

Voltages and currents will oscillate in amplitude and phase angle during power swings. The impedance measurements by distance protection relays based on these varying voltage and current signals will also vary, and can cause unwanted trip at different network locations.

Typically, a power swing blocking (PSB) function is available in modern distance relays to prevent these unwanted operations from happening.

There are many technical papers and documents describing methods for power swing detection, which will not be discussed in this paper. The focus of this paper will be the theoretical analysis of the signals that the relay senses, their behaviors, such as the signal frequency variations, and impact to the distance relay during power swing conditions. Some challenging issues in the application of the distance relays under such conditions will be discussed as well. Solutions and conclusions are discussed and supported with PSCAD or RTDS simulation testing.

## II. IMPEDANCE TRAJECTORY DURING POWER SWING

A simple power system is shown in figure below. N side is the power grid with very large inertia, and M side is a generator or a generation plant which connects to the large power grid through a transmission line L. $Z_M$ and $Z_N$ are the source impedance at the M and N side respectively.

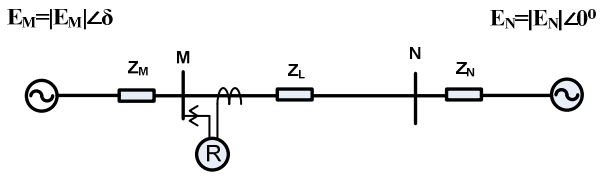


**Figure 1. Simple Power System**

It can be derived that the apparent impedance measured at the relay location (bus M) can be expressed as:

$$\boldsymbol{Z} = \frac{\boldsymbol{E_M}\cdot(\boldsymbol{Z_L}+\boldsymbol{Z_N})+\boldsymbol{E_N}\cdot\boldsymbol{Z_M}}{\boldsymbol{E_M}-\boldsymbol{E_N}} \qquad \text{(Eq 1)}$$

Because of the large inertia of the power grid, we can assume an infinite power source at N side, as such, the magnitude, phase angle and frequency of $E_N$ are kept constant during the power swing, but M side generator(s) could accelerate or decelerate depending on the condition whether loss of load or loss of generation, and as a result, the frequency of M side voltage source will change and cause the phase angle of source $E_M$ to rotate with respect to source $E_N$ at an angular speed proportional to the slip frequency (the frequency difference between these two sources).

The apparent impedance locus calculated as per Eq 1 with the variation of $E_M$ angle and the variation of K value is plotted in the figure below, where K is the ratio between the $E_M$ magnitude and $E_N$ magnitude, i.e. $K=|E_M|/|E_N|$.

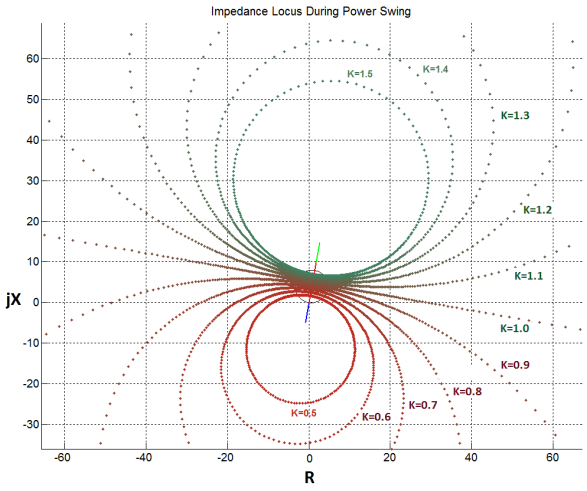


Figure 2. Impedance Locus during Power Swing, Swing Center is within zone 1 reach

For simplicity of the study, we have assumed the system is homogeneous, i.e. impedances $Z_M$, $Z_L$ and $Z_N$ have the same angle. In this plot, $Z_M=Z_N=5\Omega\angle 80^0$, $Z_L=10\Omega\angle 80^0$ in secondary Ohms are assumed.

From Figure 2, it can be seen that the apparent impedance trajectories actually traverse through the distance zone 1 Mho characteristic. Whether the impedance trajectory traverses through the distance characteristic or not will depend on whether the swing center falls inside the protected line. For example, if we change the N side source impedance $Z_N$ from 5 Ohms to 30 Ohms, the apparent impedance trajectories will not traverse through the zone 1 characteristic as shown in Figure 3 because the swing center is far outside of the zone 1 reach in this situation. The swing center is defined as the half of the total impedance, i.e. $Z_\Sigma/2=(Z_M+Z_N+Z_L)/2$, and the location where the apparent impedance locus with K=1 crosses the $Z_\Sigma$ impedance line is the exact swing center (as shown with the red square mark in Figure 3).

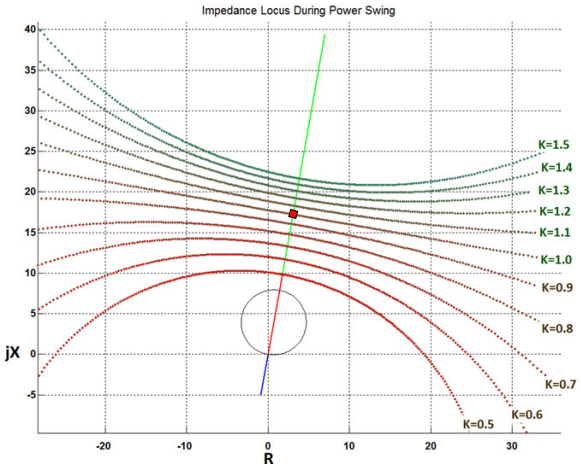


Figure 3. Impedance Locus during Power Swing, Swing Center is Outside of Zone 1 Reach

As mentioned above, methods used for the power swing detection and corresponding schemes for power swing blocking (PSB) and out of step tripping (OST) functions have been extensively discussed in the literature, and will not be discussed in this paper. We will focus on some other factors that may affect distance relay performances and applications during power swing.

## III. Theoretical Analysis to Signals that Relay Measured During Power Swing

### A. Voltage Signal

As we discussed early, power swing can be simply simulated with a frequency change at source M, while the frequency of source N is kept at nominal. Prior to the power swing, generation and load are balanced, so source $E_M$ and $E_N$ both rotate with the same angular speed proportional to the nominal frequency $f_0$. At $t=t_0$, a disturbance occurs, the balance between generation and load is broken and results in a frequency change from $f_0$ to $f_1$ at source M. For simplicity,

$E_M$ and $E_N$ are assumed to have the same amplitude, which are represented with E in the following equations.

$$e_N = \sqrt{2} \cdot E \cdot \sin(\omega_0 t) \quad \text{(Eq 2)}$$

$$e_M = \begin{cases} \sqrt{2} \cdot E \cdot sin(\omega_0 t + \beta), & t < t_0 \\ \sqrt{2} \cdot E \cdot sin(\omega_1 t + \beta), & t \geq t_0 \end{cases} \quad \text{(Eq 3)}$$

Where β is the initial phase of M side voltage source, $\omega_0=2\pi f_0$, and $\omega_1=2\pi f_1$ are the angular frequency of source N and source M respectively in radians per second. Note that N side voltage source is considered as an infinity source, in which its phase is assumed as 0 degrees and its frequency is fixed at the system nominal frequency of $f_0$. Note that the time variable shall be shifted by $t_0$ in MatLab simulation to avoid a phase step change at $t=t_0$, i.e. using $(t-t_0)$ to replace t. For the simplicity of the expression in this paper, we continue to use t as the time variable.

From these 2 equations, it can be seen that after $t=t_0$, the frequency of signal $e_M$ and $e_N$ are $f_1$ and $f_0$ respectively. However, what is the frequency at different locations in the system, for example, at bus M and bus N? Are the frequency linearly distributed along the line based on the line impedance?

To answer these questions, we need to derive the voltage signal expressions at these locations based on the two voltage source signals and the corresponding system parameters so that amplitude, phase and frequency can be extracted from such expressions.

After $t=t_0$, the instantaneous voltage signal at bus M in Figure 1 can be expressed as:

$$\begin{aligned} v_M &= e_M - \frac{e_M - e_N}{Z_\Sigma} * Z_M \\ &= \left(1 - \frac{Z_M}{Z_\Sigma}\right) \cdot e_M + \frac{Z_M}{Z_\Sigma} \cdot e_N \\ &= \left(1 - \frac{Z_M}{Z_\Sigma}\right) \cdot \sqrt{2} \cdot E \cdot \sin(\omega_1 t + \beta) + \frac{Z_M}{Z_\Sigma} \cdot \sqrt{2} \cdot E \cdot \sin(\omega_0 t) \\ &= a_1 \cdot \sqrt{2} \cdot E \cdot \sin(\omega_1 t + \beta) + a_2 \cdot \sqrt{2} \cdot E \cdot \sin(\omega_0 t) \end{aligned} \quad \text{(Eq 4)}$$

Where $a_1 = \left(1 - \frac{Z_M}{Z_\Sigma}\right)$ , $a_2 = \frac{Z_M}{Z_\Sigma}$

Based on trigonometry, Eq 4 can be rewritten as:

$$\begin{aligned} v_M &= \sqrt{2} \cdot E \cdot \sqrt{a_1^2 + a_2^2 + 2a_1 a_2 \cos((\omega_1 - \omega_0) t + \beta)} \cdot \sin(\omega_1 t + ph) \\ &= \sqrt{2} \cdot E \cdot Mag \cdot \sin(\omega_1 t + ph) \end{aligned} \quad \text{(Eq 5)}$$

Where

$$Mag = \sqrt{a_1^2 + a_2^2 + 2a_1 a_2 \cos((\omega_1 - \omega_0) t + \beta)} \quad \text{(Eq 6)}$$

$$ph = tan^{-1}\left(\frac{a_1 \sin\beta - a_2 \sin(\omega_1 - \omega_0)t}{a_1 \cos\beta + a_2 \cos(\omega_1 - \omega_0)t}\right) \quad \text{(Eq 7)}$$

Though assumptions have been made in the derivation of above equations, including homogeneous system, and the same magnitude of source $E_M$ and $E_N$, Eq 5 can be used as a general form to evaluate the voltage signal at different locations (by adjusting $a_1$ and $a_2$ values) in a 2 source power system defined in Figure 1. Based on Eq 6 and Eq 7, the magnitude and the phase angle of the voltage signal at bus M with different $a_1$ and $a_2$ values are plotted in Figure 4 and Figure 5 respectively, in which β is fixed at 30 degrees for this plot, and at $t=t_0=0.5$s, M side voltage source frequency changes to 61Hz ($f_1$) from 60Hz ($f_0$), and system starts to swing. It can be seen that the voltage magnitude oscillates with a slip frequency $f_s$ (i.e. $f_s = f_1 - f_0 = 1$ Hz). Note that the voltage magnitude won't drop to zero unless $a_1=a_2=0.5$. It is interesting to note that when $a_1=a_2=0.5$, bus M is actually the swing center. This is because when $a_1=\left(1 - \frac{Z_M}{Z_\Sigma}\right) = 0.5$, $\frac{Z_M}{Z_\Sigma}$ is equal to 0.5, which is equivalent to $Z_M=\frac{Z_\Sigma}{2}$, therefore the impedeance at bus M (measured from source $E_M$) is exatly the half of the total impedance. As mentioned in II, swing center is located at the half of the total impedance. At the swing center, the voltage magnitude becomes zero when the 2 source voltages rotate to 180 degrees apart from each other, which is exactly the same as if a 3-phase fault occurs at this location.

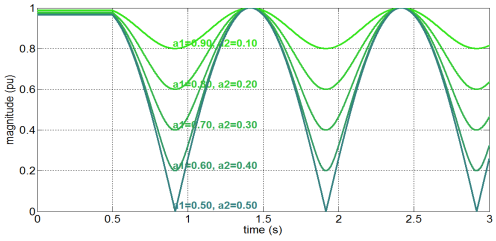


Figure 4. Voltage signal magnitude at different $a_1$ and $a_2$ values

Based on Eq 7, the phase angle of the voltage signal at bus M is plotted in Figure 5. It can be seen that it also oscillates with a slip frequency of $f_s$. As mentioned above, when $a_1=a_2=0.5$, bus M becomes the swing center. The phase angle of the voltage signal at the swing center is a special case, and it actually changes linearly at the rate of $\pi * f_s$ radians per second.

The linear change of the phase angle at the swing center can be proved from further evaluation of Eq 7. When $a_1=a_2=a$, equation 7 can be rewritten as:

$$ph = tan^{-1}\left(\frac{a \sin\beta - a \sin(\omega_1 - \omega_0)t}{a \cos\beta + a \cos(\omega_1 - \omega_0)t}\right)$$

$$= tan^{-1}\left(\frac{\sin\beta - \sin(2\pi f_s t)}{\cos\beta + \cos(2\pi f_s t)}\right)$$

$$= tan^{-1}\left(\frac{2cos\frac{\beta+2\pi f_s t}{2} sin\frac{\beta-2\pi f_s t}{2}}{2cos\frac{\beta+2\pi f_s t}{2} cos\frac{\beta-2\pi f_s t}{2}}\right)$$

$$= tan^{-1}\left(\tan(\frac{\beta-2\pi f_s t}{2})\right) \quad \text{(Eq 8 )}$$

where $f_s = f_1 - f_0$, which is the slip frequency.

Note that there are discontinuities as per Eq 8 at the points when $\frac{\beta-2\pi f_s t}{2} = k \cdot \frac{\pi}{2}, \quad k = \pm 1, 3, 5\ldots$ (odd numbers). If we omit these discontinuities, Eq 8 can be expressed with the equation shown below:

$$ph = \frac{\beta-2\pi f_s t}{2} = \frac{\beta}{2} - \pi f_s t \quad \text{(Eq 9)}$$

It can be seen from Eq 9 that the phase angle of the voltage signal at the swing center changes linearly with a rate of (-π*$f_s$) radians per second, which exactly agrees with the observation in Figure 5.

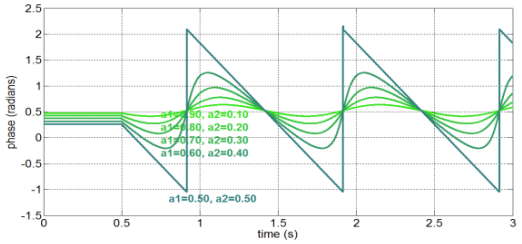


Figure 5. Voltage Signal Phase at different $a_1$ and $a_2$ values

B. Current Signal

With the same assumptions as discussed in the previous section, the cuurent signal can be expressed with:

$$i = \frac{e_m - e_n}{Z_\Sigma}$$

$$= \frac{\sqrt{2}E}{Z_\Sigma}(\sin(\omega_1 t + \beta) - \sin(\omega_0 t))$$

$$= \frac{2\sqrt{2}E}{Z_\Sigma}\sin(\frac{\omega_1-\omega_0}{2}t + \frac{\beta}{2}) * \cos(\frac{\omega_1+\omega_0}{2}t + \frac{\beta}{2})$$

$$= \frac{2\sqrt{2}E}{Z_\Sigma} * Mag\_I * \cos(2\pi\frac{f_1+f_0}{2}t + \frac{\beta}{2}) \quad \text{(Eq 10)}$$

Where $Mag\_I = \sin(2\pi\frac{f_1-f_0}{2}t + \frac{\beta}{2})$ (Eq 11)

It can be seen from Eq 10 that the frequency of the current signal is equal to the average frequency of the two source $E_M$ and $E_N$, i.e. $(f_1+f_0)/2$, and its magnitude is modulated by a sinusoildal signal at $(f_1-f_0)/2$ Hz defined in Eq 11.

The shunt capacitance on the transmission line has been omitted in this study, so the current in the system per Figure 1 is equal everywhere. Unlike voltage signal, $a_1$ and $a_2$ values do not have any impact to the current signal.

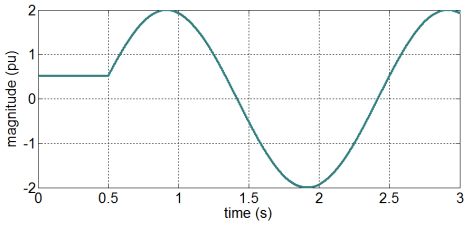


**Figure 6.** Current signal magnitude per Eq 11, which is irrelevant to $a_1$ and $a_2$ values

As per Eq 10, the phase angle of the current signal is actually a constant, which equals to $\frac{\beta}{2}, i.e.$ the half of the initial phase of source $E_M$.

C. Signal Frequency

In protection relays, voltage signals are generally preferred to be used for frequency measurement because voltage signals are more reliable, for example, their magnitudes are close to the nominal values in the normal operation condition; in the contrast, current signals are less reliable, they could be affected by loading conditions (e.g. light load), open circuits, long-lasting decaying DC on faults, harmonics contents, etc.

The frequency of the voltage signal at bus M after $t=t_0$ can be calculated by the derivative of the phase angle defined in Eq 5 and Eq 7 as shown below.

$$f = \frac{1}{2\pi}\frac{d(\omega_1 t + ph)}{dt} \quad \text{(Eq 12)}$$

Using MatLab numerical solutions for derivative calculations, the voltage signal frequency at different $a_1$ and $a_2$ values are calculated as per Eq 12 and plotted in Figure 7.

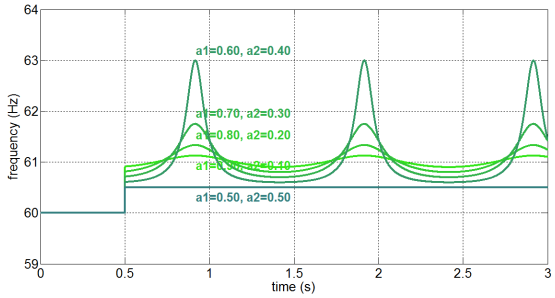


Figure 7. Voltage signal frequency at different $a_1$ and $a_2$ values

From Figure 7, it can be seen that the frequency varies nonlinearly except the voltage signal frequency at the swing

center (where $a_1$=$a_2$=0.5). The voltage signal frequency at the swing center stays constant, which is equal to the average frequency of source 1 and source 2, i.e. $f=(f_1+f_0)/2$. At non-swing-center locations, the voltage signal frequency varies in a nonlinear manner and can change dramatically when $a_1$ and $a_2$ are getting closer, in which its maximum value could be way higher than the source frequency of either side ( $f_1$ and $f_0$). It can be shown that the minimum and the maximum frequency with different $a_1$ and $a_2$ values are determined by the equations below:

$$f_{min} = f_0 + \frac{a_1(f_1-f_0)}{a_1+a_2} \qquad \text{(Eq 13)}$$

$$f_{max} = f_0 + \frac{a_1(f_1-f_0)}{a_2-a_1} \qquad \text{(Eq 14)}$$

The significant change of the frequency could adversely affect the performance of the distance protection element, which will be discussed further in later sections.

Note that the frequency of the current signal, can be calculated from the derivative of the current signal phase angle defined in Eq 10,

$$f = \frac{1}{2\pi}\frac{d(2\pi\cdot\frac{f_1+f_0}{2}\cdot t+\frac{\beta}{2})}{dt} = \frac{f_1+f_0}{2} \qquad \text{(Eq 15)}$$

It can be seen that, during power swing, the frequency of the voltage signal and the frequency of the current signal are actually different, except at the swing center. At the swing center, the frequency of the voltage signal and the frequency of the current signal are the same, which is equal to $(f_1+f_0)/2$.

Next, we would like to confirm the above analysis through the PSCAD simulation.

## IV. PSCAD Simulation Confirmation

To confirm our analysis results of the previous section, a 230kV simple power system (the same as we have defined in Figure 1), has been modeled via PSCAD simulation as shown in figure below.

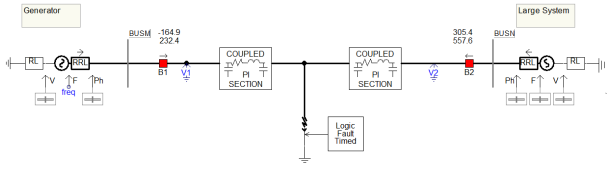


Figure 8. PSCAD Power System Model

The simulation has been implemented with the same assumption as we discussed above, including exact same voltage magnitude of $E_M$ and $E_N$, homogeneous system parameters, β (the initial phase of M side voltage source) is fixed at 30 degrees, and at t=$t_0$=0.5s, M side voltage source frequency changes to 61Hz from 60Hz.

Two particular cases have been selected for this PSCAD simulations test.

- Case 1: $Z_M$=40 ∠80$^0$, $Z_N$=20∠80$^0$, and $Z_L$=40∠80$^0$ primary Ohms, result in $a_1$=(1-$Z_M/Z_\Sigma$)=0.6 and $a_2$= $Z_M/Z_\Sigma$=0.4
- Case 2: $Z_M$=60 ∠80$^0$, $Z_N$=20∠80$^0$, and $Z_L$=40∠80$^0$ primary Ohms, result in $a_1$=(1-$Z_M/Z_\Sigma$)=0.5 and $a_2$= $Z_M/Z_\Sigma$=0.5

The voltage waveform generated from PSCAD simulation for case 1 is plotted in Figure 9 below, which agrees well with the theoretical analysis result of Figure 4. It can be seen that the voltage magnitude (envelope of the waveform) oscillates with a slip frequency of 1Hz, and the minimum and the maximum voltage peak at approximately 38kV and 188 kV respectively, which is equal to 0.2pu and 1.0 pu respectively.

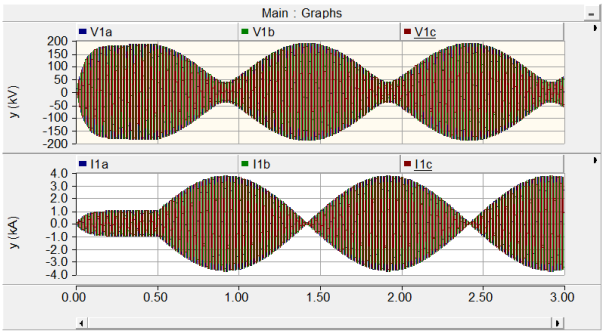


Figure 9. Voltage and Current Waveforms for Case 1($a_1$=0.6 and $a_2$=0.4) via PSCAD Simulation

The signal frequency is calculated by measuring the zero-crossing from the composed signal from the above 3-phase voltage signals through a Clark Transformation, and is plotted in Figure 10. It can also be seen that it agrees well with Figure 7.

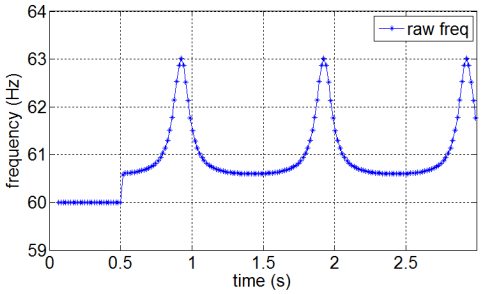


Figure 10. Measured Bus M Voltage Signal Frequency for Case 1 ($a_1$=0.6 and $a_2$=0.4)

The waveform and the frequency measurement for case 2 ($a_1$=0.5 and $a_2$=0.5, i.e. at the swing center) are plotted in

Figure 11 and Figure 12 respectively, which also agree well with the analytical result in the previous section except some frequency measurement points. At these points, there appears to be large measurement errors in the frequency plot. However, if observed carefully, the voltage signals (as shown in Figure 11) at these points are nearly zero, therefore frequency is not measurable at these points. In the frequency measurement algorithm in the relay, these measurement points will be discarded because they will fail the frequency validation checking conditions [2]. These validation checking conditions include signal magnitude, maximum/minimum frequency limit, rate of change of frequency limit, and rate of frequency acceleration limit, etc.

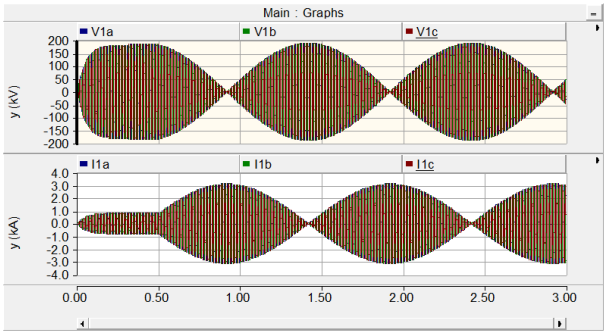


**Figure 11.** Voltage and Current Waveforms for Case 2($a_1$=0.5 and $a_2$=0.5) via PSCAD Simulation

It is interesting to mention that the frequency measurement from the current signal are actually the same as the frequency measurement from the voltage signal at the swing center shown in Figure 12 except that the discontinuity points occur at different time, because voltage signals and current signals oscillate to zero at different time as shown in Figure 11.

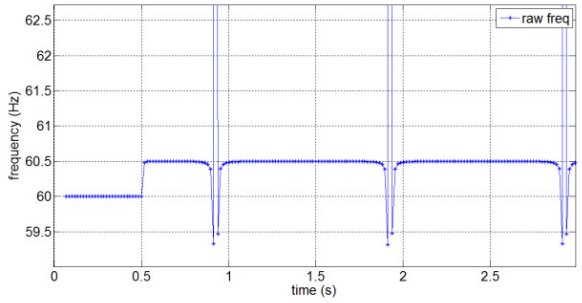


**Figure 12.** Measured Bus M Voltage Signal Frequency for Case 2 ($a_1$=0.5 and $a_2$=0.5, at the Swing Center)

## V. IMPACT TO DISTANCE RELAY PERFORMACE

The theoretical analysis to voltage and current signals during power swing was performed in III and was confirmed by PSCAD simulation in IV. Now let's see how distance relay performance can be affected by such behaviors of these signals.

### A. Frequency Tracking

Modern digital protective relays typically use variable sampling rate that tracks to the actual system frequency (frequency tracking) to reduce phasor measurement errors and avoid undesired trips during system frequency variations.

The number of samples per power cycle is always the same (for example 64 samples/cycle) with the variable sampling rate scheme (frequency tracking) regardless of the actual frequency of the input signal. In this way, the phasor magnitude and phasor angle can be estimated accurately via Fourier algorithm when system frequency varies. In a contrast, using a fixed sampling rate (without frequency tracking), the number of samples per power cycle could vary when the actual system frequency varies.

That is to say, in the data acquisition system with fixed sampling rate, the total number (say 64) of samples used in the full cycle Fourier algorithm will not exactly span the whole power cycle period when the system frequency is off from the nominal frequency, as a result, the magnitude and the angle of the estimated phasor will contain errors. Such errors could be significant if the system frequency is quite far off from the nominal frequency, and the protection relay performance could be affected.

In the variable sampling rate scheme, in order to keep the stability of the data acquisition system, sampling rate will not change too fast and too sensitive. In actual implementation, an IIR filter is typically applied to smooth out the tracking frequency variation and reduce errors during transients as shown below:

$$f_{track}(n) = (1-\alpha)\cdot f_{track}(n-1) + \alpha \cdot f(n) \qquad \text{(Eq 16)}$$

where $f_{track}(n)$ is the tracking frequency to be calculated for this step, $f_{track}(n-1)$ is the tracking frequency used in the previous step, and f(n) is the measured frequency at this step (raw frequency with validation checking), α is a real number less than 1 (e.g. 1/8) which determines the time constant of this filter. Note that frequency is calculated at every negative to positive zero crossing of the signal waveform, so the calculation step is incremented every power cycle.

As mentioned earlier, voltage signals, or some forms of combinations of voltage signals (e.g. Clarke Transformation), are generally used as the input signal for the frequency measurement. As shown above, under some system configurations, for example, in the case where the relay is located at the terminal with a weaker source ($a_1$ and $a_2$ values could be quite close in this situation), both the frequency and the rate of change of frequency of the voltage signal may experience significant changes during power swing as shown in Figure 7. In such situations, tracking

frequency may not be able to keep pace with the actual frequency because of the IIR filter time constant. For example, the system frequency and the tracking frequency for case 1 study ($a_1$=0.6 and $a_2$=0.4) are plotted in the figure below. It can be seen that the maximum difference between these two frequencies could be as high as 1.7 Hz for this case.

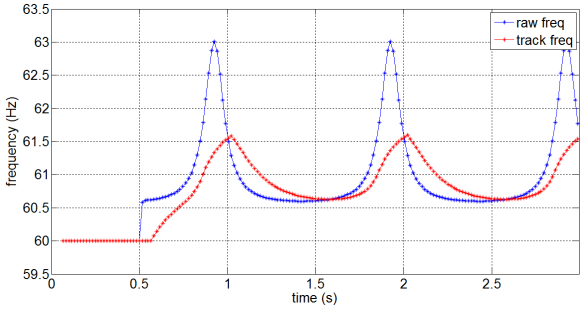


Figure 13. Raw Frequency and Tracking Frequency for Case 1 ($a_1$=0.6 and $a_2$=0.4)

Such a big difference not only causes magnitude and phase measurement errors in phasor estimation, but also causes errors in the distance memory polarization, which can directly lead to distance element mis-operation or fail to trip as discussed in the later sections.

B. Memory Polarization

Mho is the most commonly used characteristic in distance protection. The basic Mho is a circle through the origin with the reach impedance as the diameter, which is simple, reliable and inherently directional, and has been widely used for many years.

In most digital relays, Mho characteristic is realized through a phase comparator with two vectors, operating vector ($\mathbf{V_{OP}}$) and polarizing vector ($\mathbf{V_{POL}}$). Relay will trip if the absolute value of the angle difference between these two vectors is less than a limit angle (90 degrees for a circle, and less than 90 degrees for the lenticular shape).

Operating vector is defined in the equation below:

$$\boldsymbol{V_{OP} = I * Z - V} \qquad \text{(Eq 17)}$$

Where I is the loop current, $\boldsymbol{Z}$ is the impedance reach setting of the distance zone, $\boldsymbol{V}$ is the loop voltage.

There are many choices for the polarizing quantity. If loop voltage itself is selected as the polarizing quantity, the Mho characteristic is said to be "self-polarized" in which there is no dynamic expansion to the zone.

However, self-polarized distance element cannot distinguish between internal and external faults for the close-in faults when V is very small. Therefore other polarizing quantities have been selected to overcome this problem, including cross polarization with/without memory, positive sequence polarization with/without memory, etc. Among them, positive sequence voltage with a memory has been commonly used as the polarizing quantity as shown below:

$$\boldsymbol{V_{POL} = V1_{MEM}} \qquad \text{(Eq 18)}$$

Note that in Eq 18, different $V1_{MEM}$ will be used for different fault loops. For example, for AG loop, $VA\_1_{MEM}$ is used, and for AB loop, $VAB\_1_{MEM}$ is used, and so on.

With a memory polarization, the Mho characteristic will be dynamically expanded for the forward fault (origin is included) and dynamically contracted for the reverse fault (origin is excluded) as shown in Figure 14. This dynamic behavior of the Mho characteristic with memory voltage polarization is a desired feature, as such, the distance relay is able to correctly detect close-in fault, i.e. only pick up for the forward faults and not pick up for the reverse faults. [5]

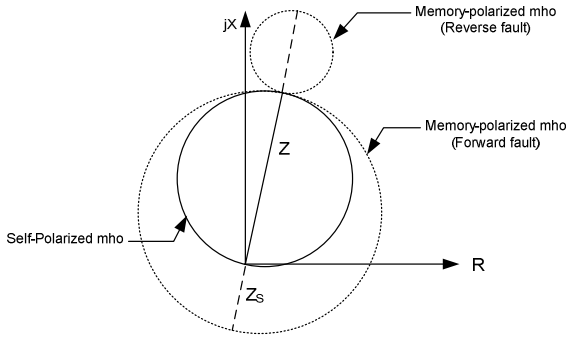


**Figure 14. Effect of Memory Polarization**

C. Directional Element with Memory Voltage

Directional element is a must for the quadrilateral characteristic which forms the bottom line of the quadrilateral shape of characteristic. Though Mho characteristic itself is inherently directional, a separate directional element can also be included for additional security. In one of the modern digital relays, the directional element is included in the Mho shape distance element and realized with the following phase comparator:

$$\boldsymbol{V_{OP} = I * Z_D} \qquad \text{(Eq 19)}$$
$$\boldsymbol{V_{POL} = V1_{MEM}} \qquad \text{(Eq 20)}$$

Where $Z_D$ is a directional element impedance setting, with a unity magnitude and a phase that defines the directional characteristic angle. Typically, a limit angle of 90 degrees is applied with this directional element comparator, but other limit angles can also be applied as well based on the application needs.

D. Impact to Distance Relay due to Memory Voltage with Power Swing

As discussed in the previous sections (B and C), memory voltage has been used as the polarizing quantity in both Mho characteristic and in the directional element. In normal situation, memory voltage is continuously updated with the actual voltage unless the actual voltage drops to below a certain level (0.8pu for example), at this time instant, the memory voltage will stop updating and be frozen.

If the actual voltage is less than a set value (10 percent for example) then the voltage prior to the fault will be remembered and used by the Mho function until the fault is cleared as indicated by reset of the Mho function. On the other hand, if the actual voltage is greater than the set value, then the voltage prior to the fault will be remembered for a short period of time (5 to 25 cycles typically) after which the voltage applied to the Mho function will adapt to the actual voltage. In general, it is best to allow the voltage be applied to a mho function to adapt to the system voltage as soon as possible following a system disturbance so that the function is in step with the system when the disturbance is cleared.[5] However, in some situations, the memory duration must be set sufficient long to ensure the correct operation of the distance elements and the directional elements, for example to overcome the possible issues caused by voltage inversion on series compensated line applications.[4]

During power swing, as showed earlier, the difference between the tracking frequency and the actual frequency could be quite big, for example, as shown in Figure 13. In such situation, the actual voltage may have shifted considerably with respect to the locked memory voltage, even during such short memory duration time. As a result, the phase angle relationship between these two quantities (actual voltage and memory voltage) used in the phase comparator is no longer valid to quantify the distance relay characteristic, and the directional element. The dynamic behavior of the Mho characteristic is also adversely affected; as such, false trip or failure to trip can both occur.

The following is an illustration of the mis-operation caused by the memory voltage during power swing on a 3-phase reverse fault. The impedance trajectory for this fault is plotted in Figure 16. It can be seen that the apparent impedance trajectory is outside the Mho characteristic on the reverse direction. However, the relay phase distance zone 1 falsely tripped in about 18 cycles from the fault inception (at t= 0.963 s) as shown in Figure **15**.

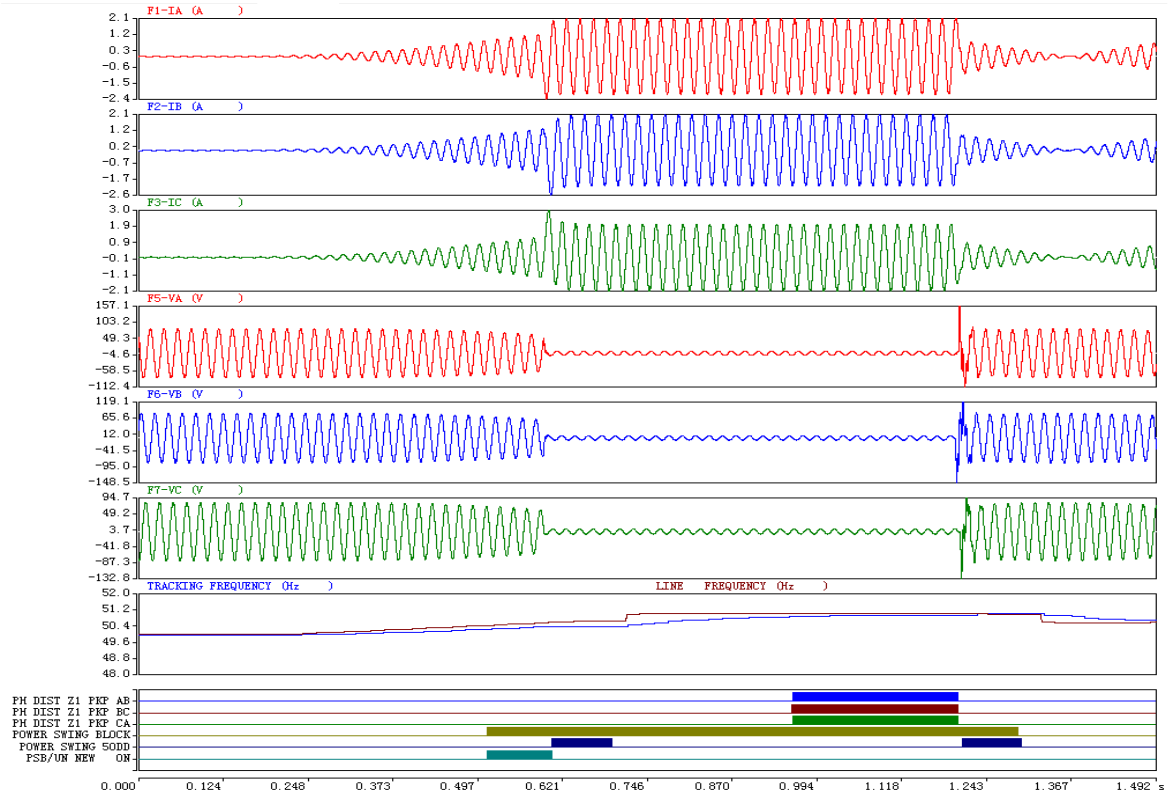


Figure 15. False Trip on Reverse Fault due to Memory Voltage during Power Swing

Note that for illustration purpose, we have purposely set memory voltage duration long enough so that actual voltage could be shifted considerably with respect to the memory voltage during this period of time (memory duration) and cause the false trip.

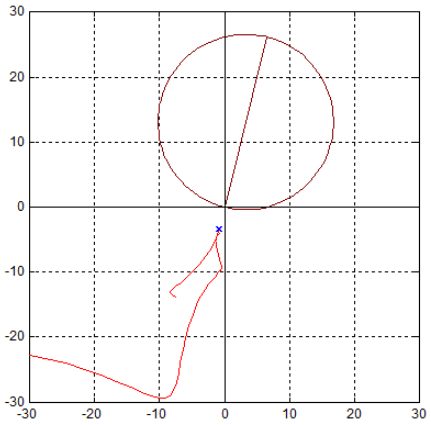


Figure 16. Impedance Trajectory of 3-Phase Reverse Fault

E. Solution to Minimize the Adverse Impact caused by Memory Voltage Polarization

Making the memory duration shorter would be a simple and an effective way to address this memory polarization issue because the memory will adapt to the actual voltage after the memory duration. This is to say, at that time, the actual voltage has not shifted too far yet from the remembered voltage within this short duration and it won't cause any issues. However, sometimes this solution may not be practical due to setting convention, system condition and testing requirement.

*1. Force Self-Polarization*

Another solution is to force using self-polarization based on the difference between the actual frequency and the tracking frequency. If the difference between the tracking frequency and the actual frequency exceeds a certain level (for example 0.2 Hz), it indicates that the tracking frequency is not able to keep pace with the actual frequency variation. This condition can be used to activate FORCE SELF-POLARIZATION input in the memory voltage logic as shown in Figure **17**. Once it's activated, self-polarization instead of memory polarization will be used in the distance elements and also in the directional elements.

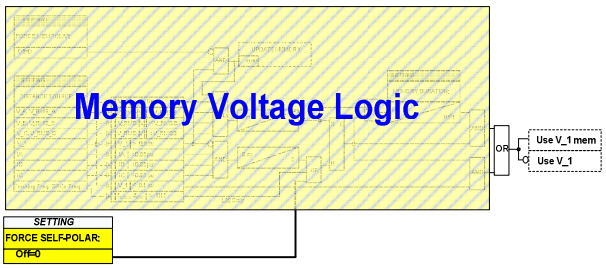


Figure 17. Force Self-Polarization

Note that even it's called self-polarized in the Memory Voltage Logic, it actually uses the actual positive sequence voltage (V_1) rather than the loop voltage as the polarizing quantity. Therefore, with this solution, it will work for all types of faults except 3-phase close-in faults.

A better solution has been developed to allow (1) continuing to use memory voltage as the polarizing quantity, and (2) memory duration can be set sufficient long based on application needs. With this solution as shown in next section, issues that were encountered before as shown in Figure **15** won't happen again.

*2. Memory Voltage Angle Compensation*

As mentioned above, frequency can be calculated by the derivative of the phase, i.e.

$$\boldsymbol{f = \frac{1}{2\pi}\frac{d\varphi}{dt}} \qquad \text{(Eq 21)}$$

Therefore, phase angle shifted in each time step due to the slip frequency between the actual frequency and the tracking frequency can be expressed as,

$$\boldsymbol{\Delta\varphi = 2\pi \cdot f_{slip} \cdot \Delta t} \qquad \text{(Eq 22)}$$

where $f_{slip} = f_{src} - f_{track}$, and $f_{src}$ is the actual frequency measured from the signal of the distance element source input. $f_{src}$ is calculated from the voltage signal if voltage is available, otherwise, it's calculated from the current signal. Note that there are a series of validation checking on the signal for frequency calculation to prevent the frequency calculation from responding to various transients. [2]

With the algorithm proposed, once the memory voltage is frozen, its angle will be automatically compensated with $\Delta\varphi$ at every time step (protection pass) with the formula as shown below.

$$\boldsymbol{\varphi = \varphi_{prev} + \Delta\varphi} \qquad \text{(Eq 23)}$$

Where $\varphi$ is the phase angle of the memory voltage at this time step, and $\varphi_{prev}$ is the phase angle of the memory voltage at the previous time step, and $\Delta\varphi$ is calculated per Eq 22.

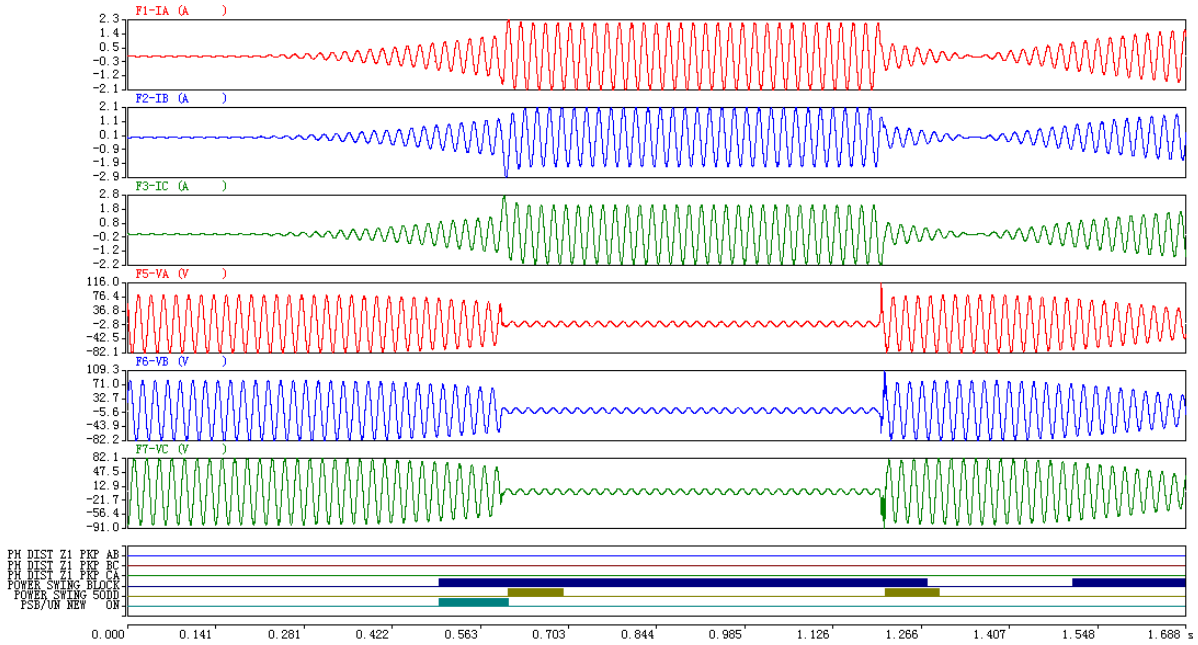


**Figure 18. No Mis-operation Occurs After Memory Voltage Angle Compensation**

With the compensation applied to the memory voltage angle per Eq 23, the previously failed cases described in D were retested, and as shown in Figure 18, there is no mis-operation now.

## VI. Other Issues in Application of Distance Relay during Power Swing

Because of the complexity and the rare occurrence of power system OOS, many utilities do not have clear performance requirements for distance relays during system OOS [3].

However, with a recent application of distance relays in Asia, it is required to test power swing combined with various fault conditions, including internal faults, external faults, evolving faults, with/without open pole conditions, different slipping frequency, etc.

The basic performance requirement to the distance relay during power swing in this application can be briefly summarized as:

- Distance relay should not operate on power swing conditions. A PSB function should be included in the distance relay and activated in such conditions to block distance elements accordingly.
- The blocking signal (PSB) to the distance elements should be removed when faults (either unbalanced or balanced) occur on the protected line at any time during the swing so that the distance elements are able to clear the faults.
- After the removal of the PSB signal from the distance elements, dependability, security and selectivity of the distance elements should be maintained. That is to say, the distance elements will not operate if the fault is external; and will reliably operate if the fault is internal.
- A proper additional delay on the distance elements is allowed after the PSB signal is removed to avoid distance elements falsely operating because the impedance trajectories of the un-faulted loops may happen to be inside the distance characteristic due to the swing.

As per the above requirement and simulation test, some issues are discussed below

### A. PSB Removal on Faults

Logic used to detect the occurrence of faults during power swing condition was based on the detection of the change of I0, I2 and I1 respectively as shown below, where K_0, K_2 and K_1 are adaptive threshold based on the average change of the past a few cycles.

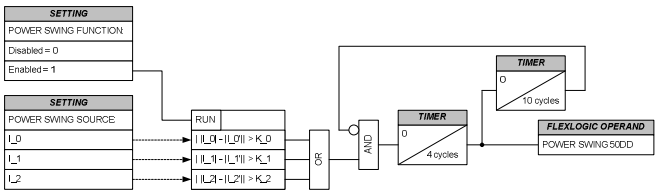


**Figure 19. Power Swing Disturbance Detection Logic**

This power swing disturbance detection logic works fine in most cases, especially for various unbalance faults. However, it may fail to detect the occurrence of 3 phase fault when the two source voltage angles are nearly 180 degrees apart. For example, $Z_M$=40 $\angle 80^0$, $Z_N$=20$\angle 80^0$, and $Z_L$=40$\angle 80^0$ primary Ohms as per the system in Figure 1 , when a solid 3-phase fault occurs in the middle of the line at t=1.8 s as shown in Figure 20.

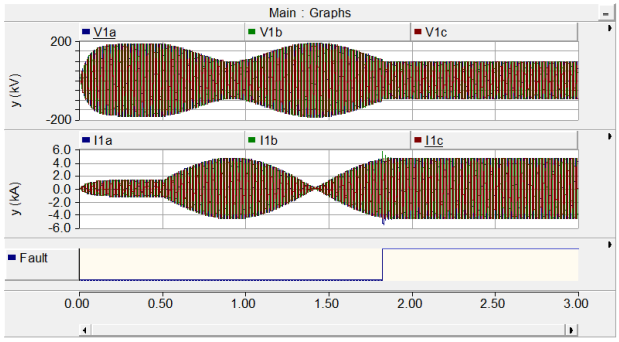


**Figure 20. 3-Phase Fault in the Middle of the line**

It can be seen from Figure 20 that there are almost no any changes on voltage and current magnitude when the fault occurs. The traditional magnitude change based disturbance detector, as showed in Figure 19, is unable to detect this fault.

Modern digital relays provide more distance protection zones than actually needed in most applications. Spare zones are typically available.

To overcome this issue, a spare zone (e.g. Zone 5) has been used to detect such 3-phase faults and remove the PSB condition accordingly. As shown in Figure 21, during power swing, impedance trajectory will traverse through the distance characteristic with a speed determined by the slip frequency between two voltage sources. However, during the 3-phase fault, the impedance trajectory will stop travelling and stay in a place determined by the fault location. Based on this, when distance zone 5 picks up on all fault loops for longer than a certain time $t_Z$, it can be concluded a 3-phase fault has occurred, as a result, PSB signal can be removed from the corresponding distance elements. The value of $t_Z$ should be determined based on the zone reach setting and the expected slowest slip frequency based on system stability studies.

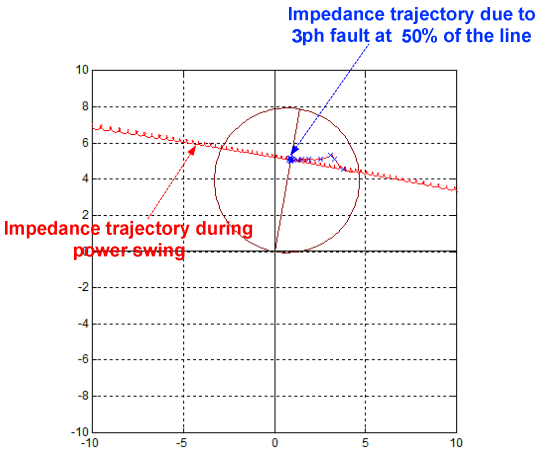


**Figure 21. Impedance trajectory of 3 phase forward fault during power swing**

The way that we just described for detection of 3-phase faults is based on the test requirement of this application, i.e. to remove the PSB signal on the previously blocked zones and allow them to trip upon fault occurrence. Actually, a time-delayed backup zone without enabling PSB, for example zone 3, can be directly used to clear these kinds of faults. The disadvantage of using the time-delayed backup zones is that the operating time of such back up zones might be slower than that of the zones (e.g. zone 1 and zone 2) previously blocked by PSB because (1) these backup zones have longer delay in order to coordinate with adjacent line zone 2, and (2) these backup zones have much larger reach settings than zone 1 and 2, as a result, the delay for these backup zones needs to be set longer because the impedance trajectory will take longer time to traverse through these zones than through zone 1 or zone 2 during power swing.

B. Security Consideration after PSB Removal

As mentioned above, PSB signal will be removed if a disturbance during power swing is detected to allow distance elements to clear the fault. However, at the time when the PSB signal is removed, the un-faulted loop impedance trajectories may happen to be located inside the distance characteristic because of the power swing. In this situation, it will lead to a false trip if the fault is external.

Modern distal relays provide powerful programming capabilities. With such capabilities, desired functionality can be easily achieved.

To prevent the possible false trip upon PSB signal removal, an additional delay is applied to distance zone 1 and zone 2 through relay programming logic. Note that this delay is applied only during power swing condition, i.e. no additional delay is applied to these zones under normal system operation conditions. The Zone1 logic is shown in

Figure 22, where POWER SWING INCOMING is an indication of power swing condition (the positive sequence impedance locus enters the inner characteristic). The delay used in this logic was based on the test requirement of this particular application and also the general guideline described in section VI.

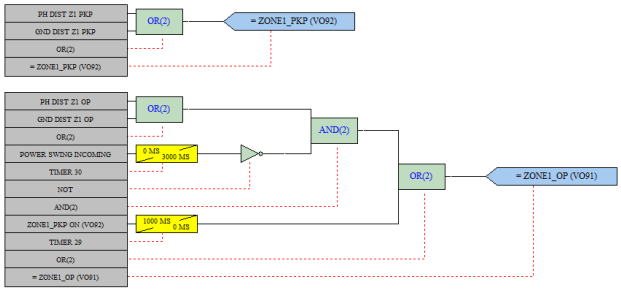


Figure 22. Zone 1 Operation Logic during Power Swing

## VII. CONCLUSION

In this paper, power swing condition has been briefly reviewed. The voltage and current signals that the distance relay measured in a 2-source power system have been analyzed. Equations have been derived to show how magnitude, phase and frequency of these signals would vary during power swing conditions. The impacts on distance relay performance due to these varying conditions have been discussed, and solutions are proposed and are summarized below:

- During power swing, frequency measured from the voltage signal and frequency measured from the current signal are not equal, which is unlike that in the normal operation condition of the power system. The former is affected by the location where the voltage measurement is taken and varies with time; the latter does not vary with time, which is equal to the average of the two source frequency.
- Memory voltage plays an important role in distance protection to distinguish between internal and external faults when voltage is close to zero and also determines the dynamic behavior of distance characteristic. However, distance element performance will be adversely affected by the memory voltage when the tracking frequency cannot keep pace with the actual frequency.
- Automatic angle compensation to the memory voltage angle based on the slip frequency between the actual and the tracking frequency is a simple and an effective way to eliminate such adverse impact on the memory voltage.
- Detection of 3 phase fault during power swing might be difficult because the fault current may be buried in the high magnitude swing current. A readily available distance spare zone in digital relay can be used to detect 3 phase fault during power swing
- Additional delay is required upon the removal of the PSB signal on distance elements to ensure security and selectivity.

Due to time constraint, the original planned studies on single pole tripping and reclosing during power swing conditions were not included in the paper, but are planned to be conducted in our future work.

## VIII. REFERENCES


[1] S. B. Wilkinson and C. A. Mathews, *Dynamic Characteristics of Mho Distance Relays*, GE Publication, GER-3720

[2] Miroslav Ristic, Ilia Voloh, Zhiying Zhang, *How Frequency Measurements can Impact Security of Frequency Elements in Digital Relays*, 37th WPRC, Spokane, 2010

[3] PSRC D-4 *Application of Overreaching Distance Relays,* IEEE/PSRC Report under http://www.pes-psrc.org/Reports

[4] GE Multilin Inc, *D60 Line Distance Protection System UR Series Instruction Manual revision 7.3x.*, Canada, Feburuary 2015

[5] J. G. Andrichak and G. E. Alexander, *Distance Relay Fundamentals*, GE Publication, GER-3966


## IX. BIOGRAPHIES

**Zhiying Zhang** received his B.Sc. and M.Sc. degrees from the North China Institute of Electric Power (now North China Electric Power University-NCEPU) and a Ph.D. degree from the University of Manitoba, Canada, all in Electrical Engineering. He has over 25 years of working experience with Electric utilities and with relay manufactures in various technical positions. Since 2007 he has been with General Electric, and currently holds the position of principal applications engineer at GE Grid Solutions in Markham, Ontario. Zhiying is a registered professional engineer in the province of Ontario, and a senior member of IEEE.

**Anil Jacques** received his B.E from university of Bombay in Electrical Engineering and has over 18 years' Experience with General Electric in Various Technical Positions, and is currently holding the position of Lead Application Engineer at GE Grid Solutions in Markham, Ontario and is involved in the development of Smart Relay platform for AJV, an Automation Joint Venture between General Electric and XD of China.

**Ilia Voloh** received his Electrical Engineering degree from Ivanovo State Power University, Russia. After graduation he worked for Moldova Power Company for many years in various progressive roles in Protection and Control field. He is currently an applications engineering manager with GE Grid Solutions in Markham Ontario, where he is involved in the development of protective relays. His areas of interest are current differential relaying, phase comparison, distance relaying and advanced communications for protective relaying. Ilia authored and co-authored more than 30 papers presented at major North America Protective Relaying conferences. He is an active member of the PSRC, and a senior member of the IEEE.